

Initiation of petroleum formation and antioxidant function – a DFT study of sulfur–sulfur bond dissociation enthalpies

Lu-Feng Zou, Kuang Shen, Yao Fu* and Qing-Xiang Guo

Department of Chemistry, University of Science and Technology of China, Hefei 230026, China

Received 12 April 2007; revised 30 May 2007; accepted 6 June 2007



ABSTRACT: Experimental studies showed that sulfur radicals play the vital role in petroleum formation.¹ Sulfur-centered radicals also exhibit activities in antioxidant functions. Here we conduct a theoretical investigation of their precursor-disulfides. By investigation into substituent effect on sulfur–sulfur bond dissociation enthalpies (S–S BDEs), we would like to find the most effective provider for sulfur radicals. In the present work, 50 alpha-substituted disulfides and 16 para-substituted aryl disulfides are studied systematically, with the general formula XS-SX or HS-SX. The substituent effect on S–S BDEs is found to be very eminent, ranging from 33.2 to 75.0 kcal/mol for alpha-substituted disulfide, and from 43.7 to 59.7 kcal/mol for para-substituted phenyl disulfides. We also evaluate the performance of 44 density functional methods to get an accurate prediction. A further study indicates that substituents play a major role in radical energies, instead of molecule energies, which is substantiated by the good linearity between XS-SX bond dissociation enthalpy (BDE) and HS-SX BDE. Copyright © 2007 John Wiley & Sons, Ltd.

Supplementary electronic material for this paper is available in Wiley InterScience at <http://www.mrw.interscience.wiley.com/suppmat/0894-3230/suppmat/>

KEYWORDS: sulfur radical; bond dissociation enthalpies; density functional methods; substituent effect; Hammett relationship

INTRODUCTION

Petroleum is mostly formed during burial in sedimentary basin through partial decomposition of kerogen. The understanding of its mechanism is critical for evaluating the potential occurrences of petroleum. Experiments show that the rate of formation depends on the concentration of sulfur radicals in the initial stages.¹ Furthermore, dimethylsulphide (DMS) becomes a star molecule since it is ready to undergo scavenge process and generate sulfur-containing radicals. Its antioxidant function for DMSP and DMS in marine algae has been discovered.² As disulfides are very promising candidates for the formation of sulfur radicals, a study of sulfur–sulfur bond dissociation enthalpies (S–S BDEs) can help understand whether and how these processes take place.

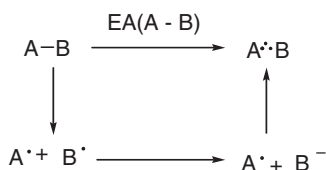
The formation and breakage of sulfur–sulfur bond is under increasing concern in biological studies such as proteins, enzymes, and antibiotics. Disulfide bridge,³ the

sulfur–sulfur bond in life, stabilize the tertiary structure of proteins and play a key role in their biological activities,^{4,5} such as the folding pathway,⁶ the coagulation process⁷ and medical study.^{8,9} Since sulfur–sulfur bonds are easy to break and form during these processes, the study of disulfides become extremely important for chemists and biologists. The activation of the heat shock protein Hsp33, a very potent molecular chaperone, is accompanied by the formation of two intramolecular disulfide bonds;¹⁰ the PhS· moiety, formed from diphenyl disulfide, could serve as an effective nucleophilic reagent, which represents the conservation of atom economy.¹¹ Besides, knowing the bond cleavage patterns in air-borne sulfur-containing pollutants is very important for environmental protection.¹² However, the experimental values are sparse because not all the S–S BDEs can be measured accurately. Therefore it is very attractive to develop some theoretical methods that can economically and precisely predict S–S BDEs and discuss into its scission capability.

The scission of the S–S bond in XS-SX molecules could occur through three different pathways¹²: (1) thermal bond dissociation, often taking place in combustion processes, (2) photochemical dissociation,

*Correspondence to: Y. Fu, Department of Chemistry, University of Science and Technology of China, Hefei 230026, China.
E-mail: fuyao@ustc.edu.cn

caused by an appropriate exciting wavelength, (3) one-electron reduction, often involved in biological systems. XS radical is obtained from the first two processes, while the third pathway leads to radical anions. The thermal bond dissociation process, which is observed in combustions, receives the most concern and will be investigated in this work. Also, through thermochemical cycle, S—S BDEs calculated for the first pathway could be used to accurately predict the electronegativity of the S—S linkage¹³:



High-level composite theoretical methods G3¹⁴, G3B3,¹⁵ and CBS-Q¹⁶ are able to give an excellent prediction of BDEs within 2 kcal/mol,^{17–20} but they are so expensive that they can only be used for systems containing less than eight non-hydrogen atoms with our current computational resources. Density functional theory (DFT) methods are much cheaper, but different performance is exhibited when dealing with different systems. Fortunately, with the continuing development, some DFTs could reach satisfactory results for calculating bond dissociation enthalpy (BDE) values in specific systems.

As early as 1992, DFT was used to predict the S—S BDE in CH₃S—SCH₃,²¹ and different *ab initio* approaches were used to obtain the bond dissociation enthalpies of HS-SH system.¹² However, since the experimental values were often randomly chosen as references for functional benchmarking, calculated S—S BDEs varies in different studies according to the selection of different theoretical approaches. What is more, only some limited types of substituted disulfide have been studied and few numbers of DFTs have been evaluated for their performances in the study of S—S BDEs. As new-generation DFTs have been developed and some of them gave satisfactory results in specific systems,^{22–26} we would like to assess their performance on the prediction of S—S BDEs. In our present study, special attention is paid upon the following two issues:

- (1) Different DFT methods are compared in order to find a method that is reasonably economical and accurate for our study.
- (2) Using the selected DFT method, S—S BDEs are computed systematically, including some typical alpha- and remote-substituted sulfur-containing molecules. Substituent effects are also studied and the best candidate for sulfide radical production is proposed accordingly.

METHOD

BDE is defined as the enthalpy change of the following reaction in gas phase at 298.15 K, 1 atm:



The enthalpy of each species can be calculated from the following equation:

$$H_{298} = E + \text{ZPE} + H_{\text{trans}} + H_{\text{rot}} + H_{\text{vib}} + RT \quad (2)$$

where ZPE is the zero point energy; H_{trans} , H_{rot} , and H_{vib} are the standard temperature correction term calculated with the equilibrium statistical mechanics with harmonic oscillator and rigid rotor approximations.

All the calculations were conducted using Gaussian 03 packages.²⁷ Calculations on radicals were performed either with a restricted open-shell reference wave function, denoted with an 'RO' prefix, or with an unrestricted-open-shell wave function, with a 'U' prefix. To obtain the global minimum structure, the conformation search by Macromodel²⁸ was used. We tried to use different DFTs in geometry optimization and found that the optimal structures are extremely similar and BDEs are only connected with single-point calculations, which is in accordance with previous study. For that reason, geometry optimizations were conducted using the (U)B3LYP/6-31+G(d) method. Each optimized structure was confirmed by the frequency calculation at the (U)B3LYP/6-31+G(d) level to rule out any imaginary vibration frequency. Single point energies were then calculated with the 6-311++G(2df, 2p) basis-set. The calculated BDEs in 298.15 K, 1 atm were corrected with (U)B3LYP/6-31+G(d) thermal correction to enthalpy (TCE) values. An optimized scaling factor²⁹ for B3LYP (0.9806) was used.

As for DFTs, Henry *et al.*³⁰ pointed out that, intriguing differences in BDEs exist between ROB3LYP and (U)B3LYP in the correlation to spin contamination. Therefore, both RODFT and UDFT single-point-energies were examined in our study. We found that ROMP2/6-311++G(2df, p) single-point energies on (U)B3LYP/6-31G(d) geometries perform well in predicting radical stabilization energies (RSEs),^{31,32} so we also tried the ROMP2 method as a comparison.

Trying to figure out which DFT is most proper for accurate prediction of the S—S BDEs, and to further examine the performance of new generation DFTs, some typical first, second, and third generation functions were used. These include B3LYP^{33,34}, B3P86³⁵, B3PW91³⁶, BHandH,³⁷ and BHandHLYP,^{34,37} mPWPW91,³⁸ PBEPBE and PBE1PBE,³⁹ B97-1,⁴⁰ B97-2,⁴¹ B98,⁴² MPW1B95,⁴³ MPWB1K,⁴³ modified Perdew-Wang 1-parameter model for kinetics (MPW1K),⁴⁴ MPW3LYP,⁴³ MPWKICIS1K,⁴⁵ TPSSTPSS,⁴⁶ TPSS1-KCIS,⁴⁷ PBE1KCIS,⁴⁸ O3LYP,^{49,50} X3LYP,⁵¹ and Boese-

Martin for kinetics (BMK)⁵². Some of the new-generation DFTs are listed as follows:

BMK

The BMK method, using an enlarged version of the HCTH/407 set⁵³ as the training set, has an accuracy in the 2 kcal/mol range for transition state barriers but, unlike previous attempts at such a functional, this improved accuracy does not come at the expense of equilibrium properties. The exchange-correlation energy is defined as follows:

$$E_{XC} = E_{X,l} + E_{X,n-l} + E_C + aE_{HF}$$

where a is defined as the mixing coefficient.

MPW1K

The MPW1K method is a hybrid Hartree-Fock density functional (HF-DF), aiming at reducing the mean unsigned error in reaction barrier heights. The one-parameter hybrid Fock-Kohn-Sham operator can be written as follows:

$$F = F^H + XF^{HFE} + (1 - X)(F^{SE} + F^{GCE}) + F^C$$

Where $X=0.428$, which minimizes the root-mean-square error of the 60 data in the database.⁴⁴

MPW1B95, MPWB1K, and MPW3LYP

The MPW1B95 and MPWB1K methods are both hybrid meta DFTs (HMDFT).⁵⁴ The one-parameter hybrid Fock-Kohn-Sham operator can be written as follows:

$$F = F^H + (X/100)F^{HFE} + [1 - (X/100)](F^{SE} + F^{GCE}) + F^{Cor}$$

In the MPW1B95 and MPWB1K models, Adamo and Barone's³⁸ mPW exchange functional is used for F^{GCE} and the Becke95 functional⁵⁵ for F^{Cor} . MPW1B95 is optimized against the AE6⁵⁶ representative atomization energy database, which is constructed for general-purpose applications in thermochemistry, while MPWB1K was optimized against the Kinetics⁵⁷ database. Thus the parameter X for MPW1B95 and MPWB1K are 31 and 44, respectively. The MPW3LYP method was constructed using the three parameters in X3LYP with the mPW exchange functional substituted for the X exchange functional.

O3LYP

The O3LYP method uses the exchange functional (OPTX) developed by Handy and Cohen⁵⁸. The

O3LYP functional is defined by the following equation⁴⁹:

$$\begin{aligned} \text{O3LYP} = & a * \text{HFX} + b * \text{LDAX} + c * \Delta\text{OPTX} \\ & + 0.19 * \text{VWN} + 0.81 * \text{LYP} \end{aligned}$$

The final results for the parameters a , b , c are 0.1661, 0.9261, and 0.8133, respectively, using the HCTH/407 set.⁵³ Compared to B3LYP, O3LYP has a reduced HF-exchange contribution, a larger coefficient multiplying OPTX compared to B88, and a different local correlation functional, VWN5 compared to VWN.

PBE1KCIS

The PBE1KCIS is a new hybrid meta GGA method. It has one parameter $X(22)$, the percentage of Hartree-Fock exchange, which was optimized against the AE6⁵⁶ database.

TPSS1KCIS

The TPSS1KCIS uses TPSS⁴⁶ as the exchange and KCIS^{59,60} correlation. TPSS1KCIS was optimized against the root mean square error (RMSE) for the MGAE109/04 Database.⁴⁷

X3LYP

The X3LYP method is constructed for general-purpose applications in thermochemistry. It is formulated following the form of the B3LYP functional:

$$\begin{aligned} E_{xc}^{X3LYP} = & a_{x0}E_X^{\text{exact}} + (1 - a_{x0})E_X^{\text{Slater}} \\ & + a_x\Delta E_x^{\text{extended}} + a_cE_c^{\text{VWN}} + (1 - a_c)E_c^{\text{LYP}} \end{aligned}$$

The extended exchange functional was proposed as follows:

$$F^X(s) = 1 + a_{x1}(F^{\text{B88}}(s) - 1) + a_{x2}(F^{\text{PW91}}(s) - 1)$$

The final results for the parameters a_{x0} , a_x , a_c are 0.218, 0.709, 0.129; a_{x1} , a_{x2} are 0.764457, 0.235543, respectively.

RESULTS AND DISCUSSION

Performance of various density functional methods

Before we calculate the S—S BDEs for substituted disulfides, it is important to ascertain that we can accurately predict them. Thus 44 DFTs (22 UDFTs and their corresponding RODFTs), including some 'new-generation' DFTs, were used to calculate the single-point

Table 1. Comparison between UB3LYP and other theoretical methods (298.15 K, 1 atm, kcal/mol)

Molecules	Exp ^a	CBS-Q ^a	G3 ^a	G3B3 ^a	ROMP2 ^a	UB3LYP ^b	UB3LYP ^b
HS-SH	64.7	64.3(−0.4)	61.6(−3.1)	61.6(−3.1)	66.2(1.5)	65.5(0.8)	58.8(−5.9)
MeS-SMe	64.0	64.8(0.8)	63.1(−0.9)	62.3(−1.7)	67.1(3.1)	62.9(−1.1)	55.5(−8.5)
PhS-SPh	51.2	—	—	—	58.2(7.0)	48.3(−2.9)	39.3(−11.9)
HS-SSH	50.0	52.8(2.8)	50.9(0.9)	50.7(0.7)	55.6(5.6)	53.2(3.2)	45.9(−4.1)
MeS-SH	65.0	64.7(−0.3)	62.4(−2.6)	62.0(−3.0)	66.8(1.8)	64.4(−0.6)	57.4(−7.6)
EtS-SEt	66.1	66.2(0.1)	64.9(−1.2)	64.0(−2.1)	69.2(3.1)	63.8(−2.3)	55.6(−10.5)
MeS-SSH	54.0	53.9(−0.1)	52.6(−1.4)	52.0(−2.0)	57.0(3.0)	53.5(−0.5)	45.6(−8.4)
MAD ^c	—	0.5	−1.4	−1.9	3.6	1.6	8.2
SD ^c	—	1.2	1.9	2.3	4.0	1.9	8.5
MD ^c	—	0.8	1.7	1.4	1.9	−0.5	−8.2

^a Taken from Reference 20.

^b Single-point energy calculations with the 6-311++G(2df, 2p) basis set on (U)B3LYP/6-31+G(d) geometries and frequencies.

^c Mean absolute deviation (MAD), mean deviation (MD), and standard deviation (SD) from experimental values.

energy using a relatively large basis set 6-311++G(2df, 2p). Seven experimental values verified by high-level *ab initio* methods in our previous work²⁰ were selected as references to evaluate DFTs. Results of the widely used B3LYP and MP2 are also listed for comparison. We can see from Table 1 that UB3LYP give prediction almost as accurate as the composite methods, which is much better than the widely used UB3LYP method. Comparison of these DFTs in terms of mean absolute deviation (MAD), mean deviation (MD), and standard deviation (SD) is shown in Table 2.

As positive and negative errors could cancel out in MD calculations, MD values could be used to evaluate

whether or not systematic deviation exists. DFTs with small MD (absolute value) could be used to calculate absolute BDEs, while those with large MD could only give relative BDEs. Sometimes even relative BDEs could not be obtained correctly.⁶¹ MD values are generally negative for these DFTs, as shown by Zhao *et al.*,⁶² especially for the widely used B3LYP and other DFTs with the LYP correlation function, which means they tend to underestimate BDEs. ROMPW1K, ROB3LYP, and ROBEPBE overestimate the BDEs, but the deviation appears to be insignificant (less than 1.5 kcal/mol), while BHandH is the only exception which systematically overestimates BDEs for both restrict or unrestricted wave

Table 2. Comparison between various DFTs^a (298.15 K, 1 atm, kcal/mol)

UDFT	MAD ^b	MD ^b	SD ^b	RODFT	MAD ^b	MD ^b	SD ^b
BMK	1.6	−0.5	1.9	MPWB1K	1.3	0.1	1.6
PBEPBE	2.1	−0.4	2.6	BMK	1.5	1.3	2.1
MPW1B95	2.1	−1.4	2.5	PBE1PBE	1.6	−0.2	1.9
MPWB1K	2.5	−2.3	2.9	MPW1B95	1.6	0.5	1.9
BHandH	2.6	2.6	3.1	MP2	1.8	0.8	2.3
PBE1KCIS	2.7	−2.4	3.2	PBE1KCIS	1.8	−0.3	2.1
mPWPW91	2.9	−2.2	3.5	B3P86	1.8	−0.4	2.2
B97-1	3.0	−2.6	3.5	B97-1	1.9	−0.5	2.3
B3P86	3.0	−2.8	3.6	mPWPW91	2.3	−0.4	2.7
PBE1PBE	3.1	−3.0	3.6	B97-2	2.4	−1.5	2.8
B97-2	3.8	−3.8	4.6	PBEPBE	2.5	1.4	3.0
B98	4.1	−4.1	4.8	MPWKCIS1K	2.5	−2.1	2.8
TPSSTPSS	4.3	−4.3	5.0	B98	2.5	−1.9	3.0
TPSS1KCIS	4.5	−4.5	5.1	TPSS1KCIS	2.6	−2.1	3.2
B3PW91	4.9	−4.9	5.4	TPSSTPSS	2.7	−2.0	3.3
MPWKCIS1K	5.1	−5.1	5.5	MPW1K	2.7	−2.4	3.0
MPW1K	6.1	−6.1	6.4	B3PW91	2.8	−2.5	3.3
MPW3LYP	7.0	−7.0	7.4	MPW3LYP	4.9	−4.9	5.4
O3LYP	7.2	−7.2	7.7	O3LYP	5.0	−5.0	5.7
X3LYP	7.7	−7.7	8.0	X3LYP	5.5	−5.5	5.9
B3LYP	8.2	−8.2	8.5	BHandH	5.5	5.5	5.7
MP2	9.0	8.7	19.7	B3LYP	6.0	−6.0	6.5
BHandHLYP	11.7	−11.7	11.9	BHandHLYP	8.2	−8.2	8.4

^a Single-point energy calculations with the 6-311++G(2df, 2p) basis set on (U)B3LYP/6-31+G(d) geometries and frequencies.

^b Mean absolute deviation (MAD), mean deviation (MD), and standard deviation (SD) from experimental values.

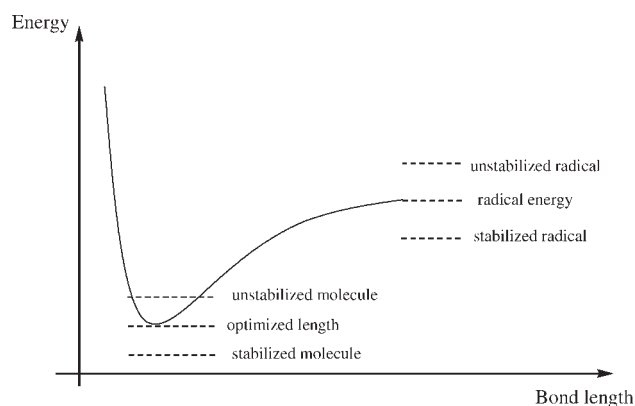


Figure 1. Relationship between bond length and molecular energy

functionals. This may attribute to the large portion of HF exchange it incorporated (50%).

Compared with MD, MAD is more reliable for the evaluation of different methods, as the positive errors are not compensated by negative errors. The SD reveals the scattering of the values. Both of them have been employed for evaluation, but for evaluation of DFTs MAD seems to be a better standard, since SD magnify large errors, which may affect the representative of the training set.

It is interesting to discover that DFTs designed for kinetic purpose outperform DFTs designed for thermochemistry. We may attribute this phenomenon to the special role of radicals: they usually act as intermediates in chemical reactions, and the dissociation procedure may be treated as a transitional state, as illustrated in Figure 1. Therefore BDE calculation is more similar to the estimation of activation energy, so kinetic DFTs are usually better choice.

An alternative explanation for this observation (thanks to the reviewer) is that newer methods with larger proportion of exact exchange tend to give better results. Previous study⁶¹ suggests that the errors in the relative BDEs were smallest for methods such as BMK and KMLYP that included the largest proportion of HF exchange, larger for those methods such as B3LYP that included a smaller proportion of HF exchange and largest for the pure DFT methods such as BLYP. Similar result is obtained in the present study, but the performance is also greatly affected by the exchange functional. UDFT with MPW or PBE exchange functional take up three places among the top four in performance (the only exception is BMK), and the same trend is seen in RODFT.

It is a long-standing controversial problem that whether restricted or unrestricted wave functions should be used for open-shell radicals. In the present work, RODFTs generally outperform UDFTs in the prediction of S—S BDEs. However, RODFTs bring in additional restrictions to open-shell wave functions, which is logically

unfeasible as Pople⁶³ mentioned⁶⁴. Moreover, RODFTs generally require more CPU time because of the difficulty in SCF convergence. So here we chose UDFTs for our calculation.

Among all these DFTs, ROMPW1K gave the least MAD (1.3 kcal/mol), followed by ROBMK and UBMK. BMK is the only one that appears to work well with both restricted and unrestricted open-shell wave functions. This proves the validity of the BMK function, probably because of the well-chosen functional form and training set.⁶⁵ Although the most accurate ROMPW1K has the least MAD and SD values, it is only slightly better than the UBMK method at the cost of much more computational time. What is more, with the same optimized geometry, SCF convergence problems, which take place more often for RODFTs than UDFTs, occur more frequently in the single-point calculation by ROMPW1K. As a result, we recommend the (U)BMK/6-311++G(2df, 2p)/(U)B3LYP/6-31+G(d) level for the prediction of S—S BDEs.

Bond dissociation enthalpies

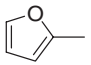
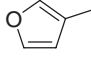
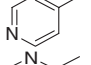
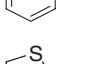
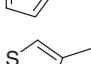
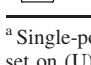
With a reliable method in hand, we try to systematically express the substituent effects on disulfides. To examine the steric repulsion effects and the electronic properties of substituents, S—S BDEs of XS-SX and HS-SX were compared. For molecules with general formula HS-SX, the steric repulsion can be ignored as the covalent radii of H are as small as 30 pm. Then the α -substituted disulfides with various types of electron demand can be divided into the following categories (Table 3):

- (1) lone-pair-donor group: F, Cl, SH, OH, OCH₃, N(CH₃)₂;
- (2) π -acceptor group: C \equiv CH, CH=CH₂, CH=CH—CH₃, C₆H₅, CHO, COCH₃, CSNH₂, furyl, pyridinyl, thienyl;
- (3) hyperconjugating group: CH₃, CH₂CH₃, *i*-Pr, *t*-Bu, *i*-Bu, and CF₃.

Among these α -substituted disulfides, S—S BDE of a heterocycle-containing molecule, 1,2-di(furan-2-yl)disulfane, is found to be the smallest (33.2 kcal/mol), which demonstrates its great potential as a sulfur-radical provider. Another possible candidate is *N*1,*N*1,*N*2,*N*2-tetramethyldisulfane-1,2-diamine, whose BDE is 34.7 kcal/mol, just 1.5 kcal/mol higher than that of 1,2-di(furan-2-yl)disulfane, but this one is simpler and the increase in BDE could be partly compensated by the uncertainty of the theoretical method.

In addition to these simple α -substituted disulfides, aromatic disulfides are of great interest in modern science, especially in polymers^{11,66–71}. Thiophenoxy radicals have gained special attention because they can help in understanding the chemistry of the related phenoxy radicals, which are well known for their antioxidant activities,⁷²

Table 3. S–S BDEs of various α -substituted disulfides^a (298.15 K, 1 atm, kcal/mol)

X	HS-SX	XS-SX
–H	65.5	65.5
–CH ₃	64.4	62.9
–C ₂ H ₅	64.9	63.8
– <i>i</i> -Pr	65.7	63.9
– <i>i</i> -Bu	64.5	61.4
– <i>t</i> -Bu	66.2	64.5
–CF ₃	67.7	67.6
–F	68.7	75.0
–Cl	62.9	60.8
–SH	53.2	41.1
–OH	61.0	57.9
–OCH ₃	60.6	56.7
–N(CH ₃) ₂	52.3	34.7
–C=CH	52.0	38.1
–CH=CH ₂	64.8	64.9
–CH=CH–CH ₃	55.6	45.3
–Ph	56.7	48.3
–CHO	67.1	67.4
–COCH ₃	64.7	63.7
–CSNH ₂	56.3	46.2
	49.4	33.2
	54.3	43.1
	60.9	56.1
	65.4	58.9
	51.2	37.8
	54.9	44.7

^a Single-point energy calculations with (U)BMK/6-311++G(2df, 2p) basis set on (U)B3LYP/6-31+G(d) geometries and frequencies.

which is recently studied by Chandra and colleagues.⁷³ Diphenyl disulfide could serve as organic intermediates; 4,4'-disulfanediyldibenzenamine is an important compound for resin additives and organic intermediates; 1,2-bis(4-chlorophenyl) disulfane could be used as intermediate for pharmaceuticals and agrochemicals. These compounds could be found in *Sumitomo Sekia Chemicals Database*.

To study the remote substituent effects on S–S BDEs in aromatic disulfides, eight molecules with representative substituents on benzene ring were selected. The calculated S–S BDEs are shown in Table 4. We can find amongst these species, the S–S BDE of 4,4'-disulfanediyldianiline is the smallest, which indicates its great potential for aromatic sulfur-radical production in medical and biological processes.

Table 4. S–S BDEs of various remote-substituted disulfides^a (298.15 K, 1 atm, kcal/mol)

Substituent	BDE _{HS-SPhX}	BDE _{XPhS-SPhX}
H	56.7	48.3
CH ₃	56.0	46.6
OCH ₃	54.6	43.7
F	56.1	47.2
Cl	56.4	47.8
NO ₂	59.7	53.2
NH ₂	53.0	40.5
CN	58.7	51.6
OH	54.7	44.3

^a Single-point energy calculations with (U)BMK/6-311++G(2df, 2p) basis set on (U)B3LYP/6-31+G(d) geometries and frequencies.

α -substituent effects on S–S BDEs

As illustrated in Figure 1, α -substituents have a two-tier impact on S–S BDEs: both stabilization and destabilization effect on either neutral molecules or radicals will influence the results. Specifically, these effects include: steric effect, Induction effect, conjugation effect, hyperconjugation effect, and isomerization.

Steric effect. This effect is caused by either steric hindrance between two substituents in XS-SX, or the repulsion between the lone electron pairs in sulfur atoms. The latter is evident because of the large span of electron clouds of sulfur. For example, the optimized dihedral angle of H–S–S–H is 90.8 degrees, much less than the H–O–O–H dihedral angle (118.2 degrees). Such effect mainly contributes to the destabilization of neutral molecules.

Induction effect. The electron donating or withdrawing properties of substituents will result in an increase or decrease in bond length and the opposite change in BDE. This effect will affect both neutral molecules and radicals, which often counteracts with each other. For that reason, it is not as noticeable in some cases.

Conjugation effect. Two kinds of conjugation effect may exist in this system, p- π conjugate and p-d feedback conjugate. The first condition plays vital roles in aromatic and unsaturated disulfides, and the second one can be found in Cl–S \cdot , HS–S \cdot , etc. Conjugation effects will stabilize the radicals greatly, but they may not be as important in neutral molecules. Therefore the net effect is the decrease of BDEs, which can be reflected clearly in our results.

Hyperconjugation effect. This effect plays a part in the S–S BDEs for α -alkyl disulfide when other effects are not significant, but hyperconjugation effect here in neutral molecules and radicals is not as important as in the stabilization of carbocations.

Isomerization. As sulfur can form either two or four valence bonds, and because of its bulky size, it is possible that S—S is polarized, especially in unsymmetrical disulfides, which in turn causes a decrease of BDE with increasing alkylation, as discussed by Izgorodina *et al.*⁶¹

These general rules can be applied to the explanation of BDEs of specific groups of compounds, as discussed in the following text.

For alkyl groups, S—S BDEs generally fall into a narrow range between 61 and 67 kcal/mol, and the relationship between BDEs and alkyl chains is random-like. This result supports our hypothesis that hyperconjugation effects are not very significant in this system. An interesting point worth mentioning is that substituent CF₃ also possesses hyperconjugation effect in that the *p* orbitals of fluorine atom are able to overlap with radical orbital. However, its strong electron-withdrawing ability may destabilize the radicals, and thus raise the S—S BDE. This increase is strangely very small (about 2 kcal/mol), which will be discussed below.

For strong electron-withdrawing groups, they will simultaneously destabilize neutral molecules and radicals, and increase the energy levels of both sides. Therefore, BDEs may not significantly change in spite of large electron-withdrawing ability. The most proper example for this hypothesis is CF₃. As mentioned above, BDE of bi-substituted molecule is even less than mono-substituted one, which cannot be explained by the common notion that more electron-withdrawing groups will further destabilize the radicals and thus increase the BDEs greater.

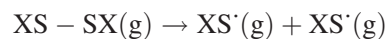
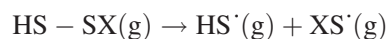
For π -acceptor groups, that is, aromatic rings, double or triple bonds, decreases in BDE generally occur, which reflected the stabilization of radicals with π -electron delocalization. It is also interesting to note that in substituted aromatic rings or heterocycles, the variances of BDEs between different substituted places are quite eminent because of remote effects.

To compare the substituent effects, relative BDEs (Δ BDEs) calculated from the following equations is used, which are listed in Table 5:

$$\Delta\text{BDE}_{\text{HS-SX}} = \text{BDE}_{\text{HS-SX}} - \text{BDE}_{\text{HS-SH}}$$

$$\Delta\text{BDE}_{\text{XS-SX}} = \text{BDE}_{\text{XS-SX}} - \text{BDE}_{\text{HS-SH}}$$

To minimize the steric repulsion between two substituents, we compared the S—S bond dissociation process of the two kinds of molecules as follows:



We can see that the radical stabilization effect (RE) for XS-SX is twice as high as that of HS-SX, a linear relationship is drawn between the two sets of data to find whether ground effect (GE) was significant. The result was shown in Fig. 2. It can be seen that the linear relationship was very good for them, with the correlation factor $r=0.99$, implying RE is additive. However, the intercept *A* was -0.58 , reflecting that the GE could not be ignored, but appears to be insignificant compared to RE. Their correlation can be described as:

$$\Delta\text{BDE}_{\text{XS-SX}} = 2\Delta\text{BDE}_{\text{HS-SX}} - 0.58$$

The greatest deviation from the equation is shown in *F* ($\Delta\text{BDE}_{\text{HS-SX}} = 3.15$, $\Delta\text{BDE}_{\text{XS-SX}} = 9.52$), NMe₂ (-13.18 and -30.82), 2-pyridinyl (-0.12 , -6.65).

Remote substituent effects on S—S BDEs

To figure out the remote substituent effects, two questions should be solved in the first place. First, does the S—S BDE obey the Hammett equation?⁷⁴⁻⁷⁷ Second, whether or not this effect could be additive? Therefore, we performed calculation on eight substituents (X) on both

Table 5. Δ BDEs of various α -substituted disulfides^a (298.15 K, 1 atm, kcal/mol)

Hyperconjugate group							
	Me	Et	<i>i</i> -Pr	<i>t</i> -Bu	<i>i</i> -Bu	CF ₃	
Usym	-1.09	-0.61	0.20	-1.04	0.72	2.15	
Sym	-2.65	-1.75	-1.65	-4.09	-0.99	2.08	
Lone-pair-donor group							
	F	Cl	SH	OH	OCH ₃	NMe ₂	
Usym	3.15	-2.66	-12.34	-4.55	-4.89	-13.18	
Sym	9.52	-4.73	-24.41	-7.58	-8.82	-30.82	
π -acceptor group: double bonds and triple bonds							
	CHO	(C=S)NH ₂	COCH ₃	C=CH	CH=CH ₂	CH=CH-CH ₃	
Usym	1.54	-9.26	-0.85	-13.52	-0.77	-9.92	
Sym	1.83	-19.31	-1.85	-27.45	-0.63	-20.22	
π -acceptor group: aromatic rings							
	Ph	2-Furyl	3-Furyl	4-Pyridinyl	2-Pyridinyl	2-Thienyl	3-Thienyl
Usym	-8.84	-16.14	-11.26	-4.58	-0.12	-14.34	-10.57
Sym	-17.18	-32.33	-22.46	-9.41	-6.65	-27.75	-20.86

^a $\Delta\text{BDE} = \text{BDE} - \text{BDE}_{\text{HS-SH}}$ (65.5 kcal/mol).

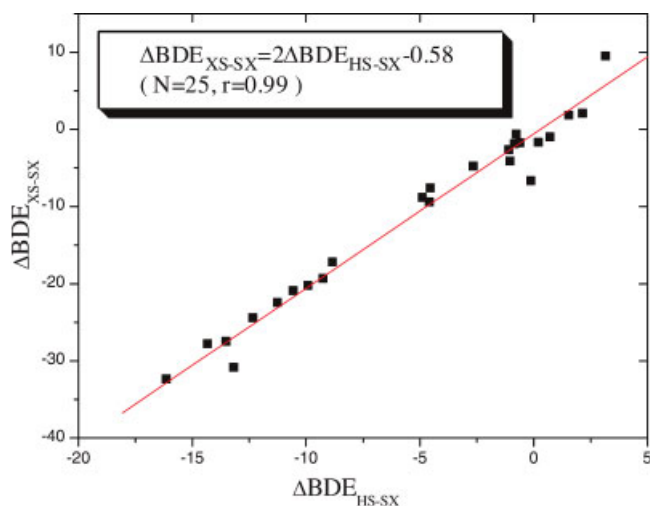


Figure 2. Linear-relationship between BDEHS-SX and BDEXS-SX for α -substituted disulfides. This figure is available in color online at www.interscience.wiley.com/journal/poc

XPhS-SPhX and HS-SPhX BDEs with the same UBMK method, and the results are listed in Table 6.

A Hammett regression between ΔBDE and substituent constants σ_p^+ was conducted to examine the remote substituent effect, as illustrated in Fig. 3.

We examined the remote substituent effect on S—S BDE with the following Hammett equation:

$$\Delta BDE = \rho^+ \sigma_p^+ + \text{Const} \quad (3)$$

Linear regression shows:

$$\Delta BDE_{X-\text{PhS}-\text{SH}} = 4.30\sigma_p^+ - 0.68 \quad (r = 0.981)$$

$$\Delta BDE_{X-\text{PhS}-\text{SPh}-X} = 8.12\sigma_p^+ - 1.74 \quad (r = 0.982).$$

According to these results, remote substituent effects on para-substituted phenyl disulfides agreed well with the Hammett equation. A positive ρ^+ value indicates that substitution of an electron-donating group decreases the S—S BDEs, while an electron-withdrawing group is thermodynamically not preferable for the bond dissociation process. In addition, the ρ^+ value of X-PhS-SPh-X is almost twice as much as that of

X-PhS-SH. Therefore it is logical to draw the conclusion that the electronic effect is additive. These results are generally in accordance with α -substituent effects.

To further understand the origin of the substituent effect, we separate it into two parts: the GE and radical effect (RE). GE reflects the influence of separating remote substituent (X) from neutral molecules, while RE reflects the influence of separating remote substituent (X) from the radical center ($\text{C}_6\text{H}_5-\text{S}^\cdot$), as show in Equations (4)–(6). GE and RE are calculated for each type of bond dissociation using the UBMK method. We also conducted Hammett regression for every GE and RE against substituent constants (σ_p^+). The results are shown in Fig. 4 and Table 6.

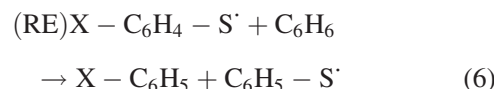
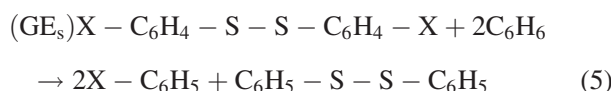
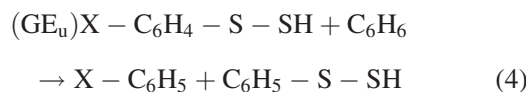


Figure 4 indicates that RE decreases sharply with the increase of the Hammett constant σ_p^+ with good linearity. This result confirms our preliminary assumption, because S^\cdot is an electron-deficient center in radicals, which will be destabilized by the introduction of electron-withdrawing groups, and thus lead to a decrease in RE. On the other hand, the substituent effect on GE is complicated. As σ_p^+ increased, GE decreases at first, reaches its minimum and then increases again. This unusual trend was shown in either symmetrically substituted molecules (GE_s in Fig. 4) or unsymmetrically substituted molecules (GE_u in Fig. 4). Nevertheless, the fluctuation is minor within the limits of error of DFTs, and thus the GE values appear to be relatively insensitive to the substituents.

By comparing the slope (ρ^+) of GE and RE, we can see that GE is not as significant as RE on S—S BDEs. This

Table 6. Remote substituent effects of para-substituent phenol-disulfides

X	σ_p^+	RE	GE_u	GE_s	$\Delta BDE_{\text{HS-SPhX}}^a$	$\Delta BDE_{\text{XPhS-SPhX}}^b$
H	0.00	0.00	0.00	0.00	0.00	0.00
CH ₃	-0.17	1.06	0.35	0.43	-0.72	-1.70
OCH ₃	-0.27	2.74	0.66	0.83	-2.08	-4.65
F	0.06	0.30	-0.28	-0.49	-0.58	-1.09
Cl	0.23	-0.14	-0.47	-0.80	-0.33	-0.52
NO ₂	0.78	-2.54	0.52	-0.26	3.06	4.83
NH ₂	-0.66	4.87	1.17	1.86	-3.70	-7.87
CN	0.66	-1.79	0.21	-0.35	2.00	3.23
OH	-0.37	2.42	0.46	0.77	-1.96	-4.07

^a Compared to $BDE_{\text{HS-SPh}} = 56.7$ kcal/mol.

^b Compared to $BDE_{\text{PhS-SPh}} = 48.3$ kcal/mol.

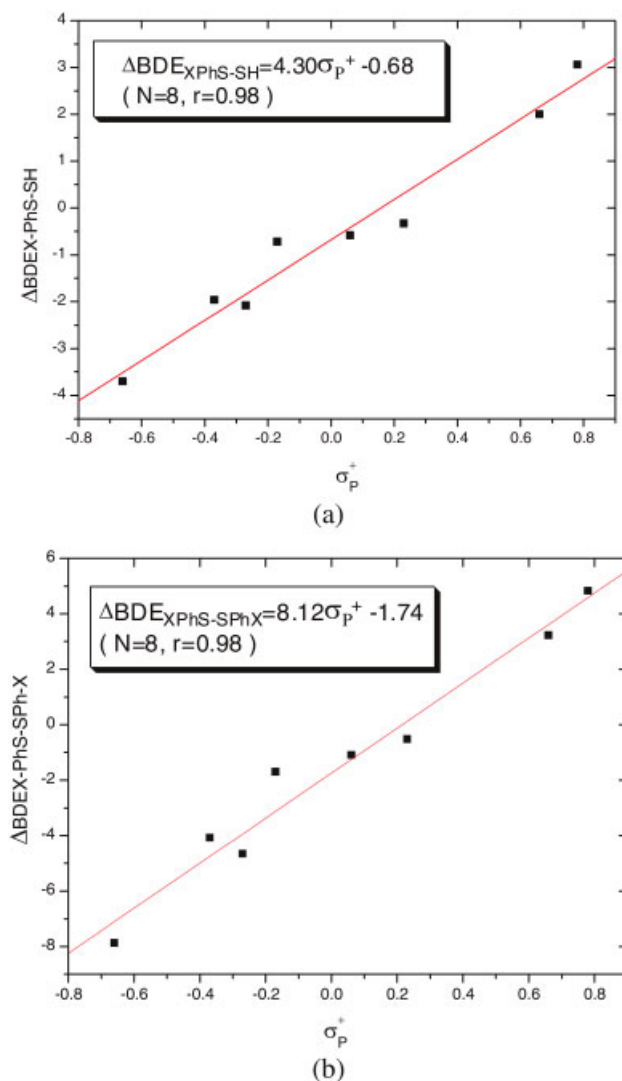


Figure 3. Remote substituent effects with Hammett relationship. This figure is available in color online at www.interscience.wiley.com/journal/poc

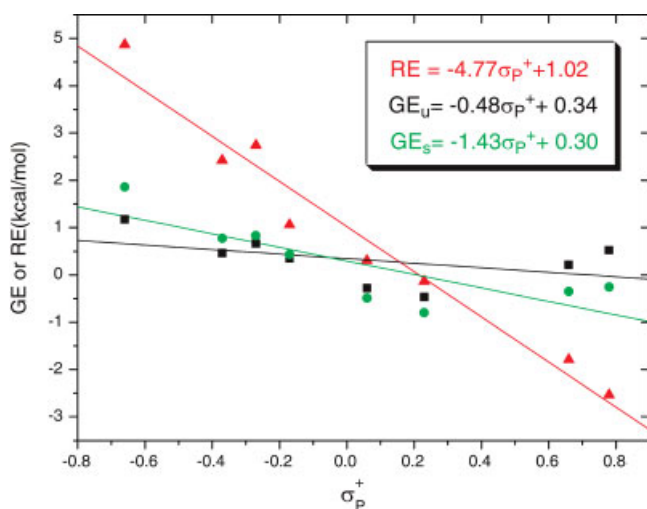


Figure 4. Ground-state effect (GE) and radical-state effect (RE). This figure is available in color online at www.interscience.wiley.com/journal/poc

explains why the substituent effects on symmetrically substituted molecules are almost twice as high as their unsymmetrical counterparts, since their RE is twice as high.

CONCLUSIONS

In the present study, we examined the performance of a variety of RODFTs and UDFTs, including several newly developed procedures in the prediction of S—S BDEs, and from these results UBMK appears to be a reasonably accurate and economical theoretical procedure. With this UBMK method in hand, we conducted systematic study on alpha and remote substituent effects on S—S BDEs. *N1,N1,N2,N2*-tetramethyldisulfane-1,2-diamine, 1,2-di(furan-2-yl)disulfane and 4,4'-disulfaneyldianiline are found to be the most effective providers for sulfur-centered radical. Subsequent study with molecules having the general formula HS-SX and XS-SX is conducted to rule out steric repulsion between substituents and to investigate into the whether the substituent effect is evident on radicals or molecules. Prominent and additive substituent effect is found, which means that stabilization of radicals plays the major part in the remote substituent effect. Results from Hammett-regression in remote-substituted molecules give further support to this conclusion.

SUPPORTING INFORMATION

The result of DFT reevaluation using larger basis set MG3 on sulfur is listed in Table S1. Calculated single-point energies of radicals and molecules with different DFTs are shown in Table S2-4. Calculated BDEs with corrected TCE are given in Table S5 and S6. Optimized Structures for molecules and radicals are given in Table S7-S11.

Acknowledgements

This study was supported by the National Natural Science Foundation of China (No.20602034). We thank Super-computer Center of University of Science and Technology of China for the computational resources. We also thank Professor Boese and Professor Martin for designing the BMK method and Professor Truhlar's group for designing most of the new-generation DFTs.

REFERENCES

- Lewan MD. *Nature* 1998; **391**: 164–166.
- Sunda W, Kieber DJ, Kiene RP, Huntsman S. *Nature* 2002; **418**: 317–320.
- Lescic I, Zehl M, Muller R, Vukelic E, Abramic M, Allmaier G, Kojic-Prodic B. *J. Biol. Chem.* 2004; **385**: 1147–1156.

4. Fu Y, Lin BL, Song KS, Liu L, Guo QX. *J. Chem. Soc. Perkin Trans. 2*; 2002; 1223–1230.
5. Perry LJ, Wetzel R. *Science* 1984; **226**: 555–557.
6. Kim J, Robinson AS. *Protein Sci.* 2006; **15**: 1791–1793.
7. Gale AJ, Radtke KP, Cunningham MA, Chamberlain D, Pellequer JL, Griffin JH. *J. Thromb. Haemost.* 2006; **4**: 1315–1322.
8. Batista CVF, del Pozo L, Zamudio FZ, Contreras S, Becerril B, Wanke E, Possani LD. *J. Chromatogr. B* 2004; **803**: 55–66.
9. Liu L, Bennett CS, Wong CH. *Chem. Commun.* 2006; 21–33.
10. Barbirz S, Jakob U, Glocker MO. *J. Biol. Chem.* 2000; **275**: 18759–18766.
11. Chakraborti AK, Nayak MK, Sharma L. *J. Org. Chem.* 2002; **67**: 1776–1780.
12. Benassi R, Taddei F. *J. Phys. Chem. A* 1998; **102**: 6173–6180.
13. Braidia B, Hiberty PC. *J. Phys. Chem. A* 2003; **107**: 4741–4747.
14. Curtiss LA, Raghavachari K, Redfern PC, Rassolov V, Pople JA. *J. Chem. Phys.* 1998; **109**: 7764–7776.
15. Li MJ, Liu L, Fu Y, Guo QX. *J. Phys. Chem. B* 2005; **109**: 13818–13826.
16. Ochterski JW, Petersson GA, Wiberg KB. *J. Am. Chem. Soc.* 1995; **117**: 11299–11308.
17. Qi XJ, Feng Y, Liu L, Guo QX. *Chin. J. Chem.* 2005; **23**: 194–199.
18. Feng Y, Liu L, Wang JT, Huang H, Guo QX. *J. Chem. Inf. Comput. Sci.* 2003; **43**: 2005–2013.
19. Song KS, Liu L, Guo QX. *Tetrahedron* 2004; **60**: 9909–9923.
20. Zou L-F, Fu Y, Shen K, Guo Q-X. *Theochem* 2007; **807**: 87–92.
21. Fournier R, Depristo AE. *J. Chem. Phys.* 1992; **96**: 1183–1193.
22. van der Wijst T, Guerra CF, Swart M, Bickelhaupt FM. *Chem. Phys. Lett.* 2006; **426**: 415–421.
23. Li AHT, Chao SD. *Phys. Rev. A* 2006; **73**: 016701.
24. Liu YC, Zhao WY. *Acta Chim. Sin.* 1991; **49**: 615–620.
25. Brom JM, Schmitz BJ, Thompson JD, Cramer CJ, Truhlar DG. *J. Phys. Chem. A* 2003; **107**: 6483–6488.
26. Brothers EN, Merz KM. *J. Phys. Chem. A* 2004; **108**: 2904–2911.
27. Frisch GWT MJ, Schlegel HB, Scuseria GE, Robb MA, Cheeseman JR, Montgomery JA, Jr, Vreven T, Kudin KN, Burant JC, Millam JM, Iyengar SS, Tomasi J, Barone V, Mennucci B, Cossi M, Scalmani G, Rega N, Petersson GA, Nakatsuji H, Hada M, Ehara M, Toyota K, Fukuda R, Hasegawa J, Ishida M, Nakajima T, Honda Y, Kitao O, Nakai H, Klene M, Li X, Knox JE, Hratchian HP, Cross JB, Bakken V, Adamo C, Jaramillo J, Gomperts R, Stratmann RE, Yazyev O, Austin AJ, Cammi R, Pomelli C, Ochterski JW, Ayala PY, Morokuma K, Voth GA, Salvador P, Dannenberg JJ, Zakrzewski VG, Dapprich S, Daniels AD, Strain MC, Farkas O, Malick DK, Rabuck AD, Raghavachari K, Foresman JB, Ortiz JV, Cui Q, Baboul AG, Clifford S, Cioslowski J, Stefanov BB, Liu G, Liashenko A, Piskorz P, Komaromi I, Martin RL, Fox DJ, Keith T, Al-Laham MA, Peng CY, Nanayakkara A, Challacombe M, Gill PMW, Johnson B, Chen W, Wong MW, Gonzalez C, Pople JA. *Gaussian 03, Revision D.01*. Gaussian, Inc.: Wallingford CT, 2004.
28. Fariborz NGJR, Wayne CC, Rob L, Mark L, Craig C, George C, Thomas H, Still WC. *J. Comput. Chem.* 1990; **11**: 440–467.
29. Scott AP, Radom L. *J. Phys. Chem.* 1996; **100**: 16502–16513.
30. Henry DJ, Parkinson CJ, Mayer PM, Radom L. *J. Phys. Chem. A* 2001; **105**: 6750–6756.
31. Wang YM, Zhou C, Fu Y, Liu L, Guo QX. *Chin. J. Org. Chem.* 2005; **25**: 1398–1402.
32. Fu Y, Yu TQ, Wang YM, Liu L, Guo QX. *Chin. J. Chem.* 2006; **24**: 299–306.
33. Becke AD. *J. Chem. Phys.* 1993; **98**: 5648–5652.
34. Lee C, Yang W, Parr RG. *Phys. Rev. B* 1988; **37**: 785.
35. Perdew JP. *Phys. Rev. B* 1986; **34**: 7406.
36. Perdew JP, Chevary JA, Vosko SH, Jackson KA, Pederson MR, Singh DJ, Fiolhais C. *Phys. Rev. B* 1992; **46**: 6671.
37. Becke AD. *J. Chem. Phys.* 1993; **98**: 1372–1377.
38. Adamo C, Barone V. *J. Chem. Phys.* 1998; **108**: 664–675.
39. Lee IH, Martin RM. *Phys. Rev. B* 1997; **56**: 7197–7205.
40. Cohen AJ, Tantirungrotechai Y. *Chem. Phys. Lett.* 1999; **299**: 465–472.
41. Wilson PJ, Bradley TJ, Tozer DJ. *J. Chem. Phys.* 2001; **115**: 9233–9242.
42. Bienati M, Adamo C, Barone V. *Chem. Phys. Lett.* 1999; **311**: 69–76.
43. Zhao Y, Truhlar DG. *J. Phys. Chem. A* 2004; **108**: 6908–6918.
44. Lynch BJ, Fast PL, Harris M, Truhlar DG. *J. Phys. Chem. A* 2000; **104**: 4811–4815.
45. Fu Y, Dong XY, Wang YM, Liu L, Guo QX. *Chin. J. Chem.* 2005; **23**: 474–482.
46. Staroverov VN, Scuseria GE, Tao JM, Perdew JP. *J. Chem. Phys.* 2003; **119**: 12129–12137.
47. Zhao Y, Lynch BJ, Truhlar DG. *Phys. Chem. Chem. Phys.* 2005; **7**: 43–52.
48. Zhao Y, Truhlar DG. *J. Chem. Theory Comput.* 2005; **1**: 415–432.
49. Hoe WM, Cohen AJ, Handy NC. *Chem. Phys. Lett.* 2001; **341**: 319–328.
50. Cohen AJ, Handy NC. *Mol. Phys.* 2001; **99**: 607–615.
51. Xu X, Goddard WA. *Proc. Natl. Acad. Sci. U. S. A.* 2004; **101**: 2673–2677.
52. Boese AD, Martin JML. *J. Chem. Phys.* 2004; **121**: 3405–3416.
53. Liu L, Shao XG, Cai WS, Jiang Y, Pan ZX. *Chin. Chem. Lett.* 1998; **9**: 203–206.
54. Perdew JP. *Phys. Rev. Lett.* 1985; **55**: 1665.
55. Becke AD. *J. Chem. Phys.* 1997; **107**: 8554–8560.
56. Lynch BJ, Truhlar DG. *J. Phys. Chem. A* 2003; **107**: 8996–8999.
57. Zhao Y, Lynch BJ, Truhlar DG. *J. Phys. Chem. A* 2004; **108**: 2715–2719.
58. Handy NC, Cohen AJ. *Mol. Phys.* 2001; **99**: 403–412.
59. Rey J, Savin A. *Int. J. Quantum Chem.* 1998; **69**: 581–590.
60. Toulouse J, Savin A, Adamo C. *J. Chem. Phys.* 2002; **117**: 10465–10473.
61. Izgorodina EI, Coote ML, Radom L. *J. Phys. Chem. A* 2005; **109**: 7558–7566.
62. Zhao Y, Pu JZ, Lynch BJ, Truhlar DG. *Phys. Chem. Chem. Phys.* 2004; **6**: 673–676.
63. Pople JA, Gill PMW, Handy NC. *Int. J. Quantum Chem.* 1995; **56**: 303–305.
64. Li XS, Liu L, Schlegel HB. *J. Am. Chem. Soc.* 2002; **124**: 9639–9647.
65. Liang ZA, Meng YZ, Truhlar DG. *J. Chem. Theory Comput.* 2006; **2**: 364–382.
66. Meng YZ, Liang ZA, Lu YX, Hay AS. *Polymer* 2005; **46**: 11117–11124.
67. Liang ZA, Meng YZ, Li L, Du XS, Hays AS. *Macromolecules* 2004; **37**: 5837–5840.
68. Liu L, Breslow R. *Bioorg. Med. Chem.* 2004; **12**: 3277–3287.
69. Xu LZ, Xu FL, Li K, Lin Q, Zhou K. *Chin. J. Chem.* 2005; **23**: 1421–1424.
70. Aslam M, Bandyopadhyay K, Vijayamohan K, Lakshminarayanan V. *J. Colloid Interface Sci.* 2001; **234**: 410–417.
71. Modelli A, Jones D. *J. Phys. Chem. A* 2006; **110**: 10219–10224.
72. Chandra AK, Nam PC, Nguyen MT. *J. Phys. Chem. A* 2003; **107**: 9182–9188.
73. Nam PC, Nguyen MT, Chandra AK. *J. Phys. Chem. A* 2006; **110**: 10904–10911.
74. Hansch C, Leo A, Taft RW. *Chem. Rev.* 1991; **91**: 165–195.
75. Fu Y, Liu L, Lin BL, Yi M, Cheng YH, Guo QX. *J. Org. Chem.* 2003; **68**: 4657–4662.
76. Liu L, Fu Y, Liu R, Li RQ, Guo QX. *J. Chem. Inf. Comput. Sci.* 2004; **44**: 652–657.
77. Exner O, Bohm S. *Curr. Org. Chem.* 2006; **10**: 763–778.